



Available online at [www.sciencedirect.com](http://www.sciencedirect.com)  
**jmr&t**  
 Journal of Materials Research and Technology  
 journal homepage: [www.elsevier.com/locate/jmrt](http://www.elsevier.com/locate/jmrt)



## Original Article

# Compressive strength development and durability properties of high volume slag and slag-fly ash blended concretes containing nano-CaCO<sub>3</sub>



Anwar Hosan, Faiz Uddin Ahmed Shaikh\*

School of Civil and Mechanical Engineering, Curtin University, Perth, Australia

## ARTICLE INFO

### Article history:

Received 21 August 2020

Accepted 3 January 2021

Available online 6 January 2021

### Keywords:

High volume slag  
 High volume slag-fly ash blend  
 Nano calcium carbonate  
 Compressive strengths  
 Durability properties  
 Drying shrinkage  
 Microstructure

## ABSTRACT

This paper presents the effect of nano-CaCO<sub>3</sub> (NC) on the compressive strengths and durability properties of high volume slag (HVS) and high volume slag-fly ash (HVS-FA) blended concretes. The study examined the improvement in early and later age compressive strengths and durability properties such as sorptivity, volume of permeable voids, rapid chloride penetration and drying shrinkage of HVS concrete containing 69% blast furnace slag (BFS) and HVS-FA concrete containing combined BFS and fly ash (FA) content of 69% due to the addition of 1% NC. Results show that the addition of 1% NC improved the compressive strengths of HVS and HVS-FA concretes significantly by 43% and 28%, respectively at 3 days compared to the control HVS and HVS-FA concretes without NC and exceeded the compressive strengths of control OPC concrete at later ages. It is also found that 1% NC inclusion reduced the water sorptivity of HVS and HVS-FA concretes reasonably after 28 days of curing and reduction is greater after 90 days of curing exhibited comparable water sorptivity to OPC concrete. Significant improvement is also observed in reducing the volume of permeable voids and controlling the drying shrinkage strain at early age as well as later ages of both HVS and HVS-FA concretes due to 1% NC inclusion. Outstanding resistance against chloride ion penetration is also observed in HVS and HVS-FA concretes due to addition of 1% NC to the very low level of chloride ion penetration according to ASTM standard. SEM and EDS analysis revealed a denser microstructure of paste and interfacial transition zone (ITZ) around aggregates.

© 2021 The Author(s). Published by Elsevier B.V. This is an open access article under the CC BY-NC-ND license (<http://creativecommons.org/licenses/by-nc-nd/4.0/>).

## 1. Introduction

Concrete is the key part of rapid development of the modern world and the use of ordinary Portland cement (OPC) is unavoidable in the concrete production. Studies show about

115–180% increase in OPC demand in 2020 compared to 1990s and projected to be climbed to 400% by 2050 [1]. However, every tonne of OPC manufacturing consumes around 1.5 tonnes of raw materials and releases roughly 0.9 tonne of carbon dioxide (CO<sub>2</sub>) which is about 7% of the total global emission of

\* Corresponding author.

E-mail address: [s.ahmed@curtin.edu.au](mailto:s.ahmed@curtin.edu.au) (F.U.A. Shaikh).

<https://doi.org/10.1016/j.jmrt.2021.01.001>

2238-7854/© 2021 The Author(s). Published by Elsevier B.V. This is an open access article under the CC BY-NC-ND license (<http://creativecommons.org/licenses/by-nc-nd/4.0/>).

**Table 1 – Physical properties and chemical compositions of Ordinary Portland Cement (OPC), Blast Furnace Slag (BFS), Class F Fly Ash (FA) and nano-CaCO<sub>3</sub> (NC).**

		Cement	Slag	Fly-ash	nano-CaCO <sub>3</sub>
Chemical composition (%)	CaO	64.39	41.20	4.30	97.8 <sup>a</sup>
	SiO <sub>2</sub>	21.10	32.5	51.11	—
	Al <sub>2</sub> O <sub>3</sub>	5.24	13.56	25.56	—
	Fe <sub>2</sub> O <sub>3</sub>	3.10	0.85	12.48	0.02 <sup>a</sup>
	MgO	1.10	5.10	1.45	0.5 <sup>a</sup>
	MnO	—	0.25	0.15	—
	K <sub>2</sub> O	0.57	0.35	0.7	—
	Na <sub>2</sub> O	0.23	0.27	0.77	—
	P <sub>2</sub> O <sub>5</sub>	—	0.03	0.88	—
	TiO <sub>2</sub>	—	0.49	1.32	—
	SO <sub>3</sub>	2.52	3.20	0.24	—
	LOI	1.22	1.11	0.57	—
Physical properties	Particle size	10–30% ≤ 7 μm	40% < 10 μm	50% < 10 μm	15–40 nm
	Surface area (m <sup>2</sup> /g)	—	—	—	40
	Specific gravity	2.5 to 3.2	2.6	—	—

<sup>a</sup> Information provided by supplier.

CO<sub>2</sub> into the atmosphere [2–6]. A number of research have been conducted to reduce the use of OPC in large volume (>50%) in concrete and replace it with other supplementary cementitious materials (SCM) such as blast furnace slag (BFS), fly ash (FA), rice husk ash (RHA), silica fume (SF), metakaolin, etc. to produce sustainable concrete with low carbon footprint [7–14]. Duran Atiş and Bilim [7] reported that the compressive strength of concrete containing 60% BFS as partial replacement of OPC is equivalent to that of control OPC concrete at 28 days. However, Güneyisi and Gesoğlu [8] reported a systematic decrease in compressive and splitting tensile strengths with the increase in BFS contents at the early ages. Similarly, Oner and Akyuz [9] observed lower early ages strength of high volume BFS concrete than the control concrete. However, the compressive strength is increased with curing and exceeded the control concrete after one year of curing. They also noted highest compressive strength in concrete containing 55% BFS. Wainwright and Rey [10] also observed improved properties of concrete containing 55% BFS. Aghaeipour and Madhkan [11] found that concrete containing 60% slag led to reduced water absorption. On the other hand, few research examined the properties of BFS and FA blended concrete and reported very low early age strengths, increased initial and final setting time and notable drying shrinkage due to slow pozzolanic reaction of BFS and FA [12–14].

Recently, the use of various nano materials as partial replacement of cement in concrete gained acceptance due to their fast pozzolanic and hydration reactions. It is reported that nano materials can be used as a reacting agent to improve early age strengths, control of setting times and reduce autogenous shrinkage of cementitious mixtures by accelerating hydration process [15–22]. Use of various nano materials also show improvement in mechanical and durability properties environmental friendly concretes containing high volume FA as partial replacement of OPC [23–27].

In all the above studies on use of BFS in concrete it can be seen that the BFS was used up to 60% as partial replacement of cement. However, in order to increase the environmental friendliness of concrete and to reduce its carbon footprint significantly the replacement levels of cement by BFS or other

by-products e.g. FA need to be increased significantly without compromising the mechanical and durability properties of concrete. Recently, authors [28] studied the effect of various high volume BFS content from 60% to 90% as partial replacement of cement as well as combined BFS-FA content up to 90% as partial replacement of cement on 28 days compressive strength of cement mortar. The effect of various nano- CaCO<sub>3</sub> (NC) contents of 1–4% (by wt.) in the above mortars is also evaluated. Results show that the compressive strength is decreased with increase in BFS and BFS-FA contents from 70 to 90%. However, with addition of NC the compressive strength of above mortars containing BFS and BFS-FA is increased compared to their respective control mortars. Promising results are obtained at BFS and BFS-FA content of 70% with the addition of 1% NC whose compressive strength exceeded that of control cement mortar. Microstructural analysis also showed densified microstructure of mortars containing BFS and BFS-FA content of 70% with the addition of 1% NC than that of control cement mortar. However, understanding of durability properties of above environmentally friendly concretes will be very useful for their wide application in the industry. Therefore, this study aims to extend the above findings and understanding in [28] through investigating the effect of 1% nano-CaCO<sub>3</sub> on the compressive strength development of concretes containing 70% BFS and combined BFS-FA content of 70% as partial replacement of OPC from 3 days to 6 months and durability properties such as sorptivity, volume of permeable voids (VPV), rapid chloride permeability test (RCPT) and drying shrinkage of the above concretes. Durability properties are measured at 28 and 90 days. Above results are also bench marked with the control cement concrete. Microstructural analysis in terms of scanning electron microscope (SEM) of cement matrix containing 70% BFS and combined BFS-FA content of 70% as partial replacement of cement with and without 1% NC as well as interfacial transition zone (ITZ) between aggregates and matrix of above concretes are also performed to understand the role of NC on densification of the ITZ and matrix of above concretes and their influence on the durability properties and compressive strength development.

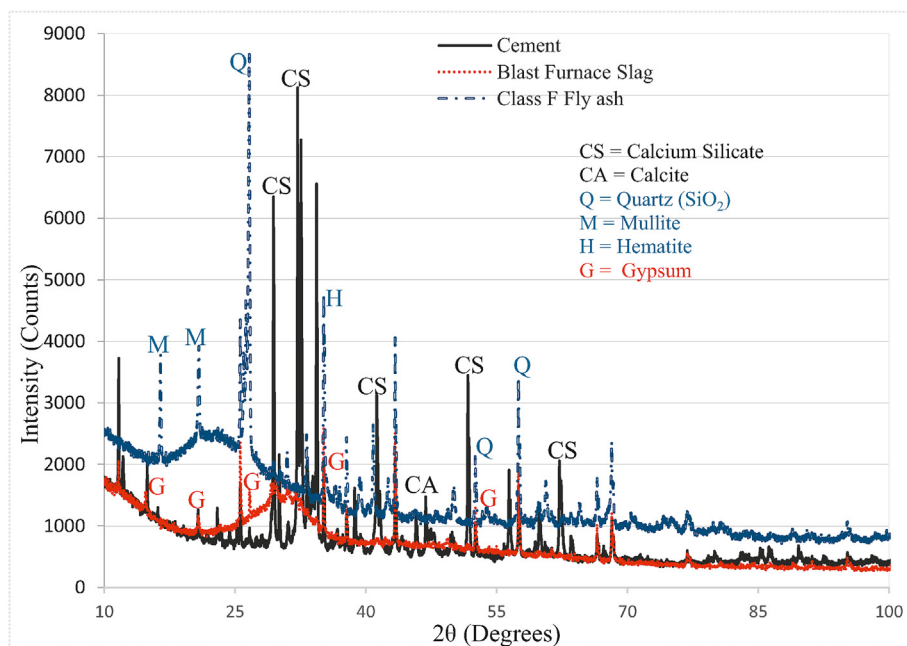


Fig. 1 – XRD analysis of Cement, blast furnace slag and fly ash.

## 2. Outline of the experiments

### 2.1. Materials

Ordinary Portland Cement Type I (OPC) used in this study was purchased from a local cement company. The blast furnace slag (BFS) was supplied by BGC cement company of Western Australia and class F fly ash (FA) was provided by Eraring power station of NSW, Australia. All coarse and fine aggregate used in this study was sourced locally ensuring the ASTM C127 standard quality. Aggregates were soaked for at least 24 h to achieve saturated and surface dry (SSD) condition. Dry nano- $\text{CaCO}_3$  (NC) powder with an average particle size of 15–40 nm, specific surface areas of  $40 \text{ m}^2/\text{g}$  and calcite content of 97.8% was purchased from Nanostructured and Amorphous Materials, Inc. of USA. Tap water was used in all mixes and a naphthalene sulphonate based superplasticizer was used to maintain the workability by measuring slump for all mixes. Physical and chemical properties of all cementitious materials are given in Table 1. Figs 1–2 shows the X-ray diffraction (XRD) analysis of cement, BFS, FA and nano- $\text{CaCO}_3$ . It is clear that nano- $\text{CaCO}_3$  was less amorphous than BFS and FA. However, among both supplementary cementitious materials, the BFS is more amorphous with amorphous content of 97.5% compared to that of 67.8% for FA based on quantitative XRD analysis results [28].

### 2.2. Mix proportions

All the concrete mixes were designed with a total binder quantity of  $400 \text{ kg/m}^3$  and a constant water/binder ratio of 0.4. However, superplasticizer was used when needed to maintain the workability of the mixes with a target slump of 100–120 mm. Coarse and fine aggregates mass and ratios were

kept constant for all mixes. Table 2 shows the mix proportions of all mixes. A designated ID was given for each mix considering binder name and amount present on the mixes. For example, 70BFS means a mix containing 70% BFS and 30% OPC of total binder.

### 2.3. Sample preparation

Concrete mixes were prepared in a pan mixer at ambient temperature. First, all dry ingredients such as cement, coarse aggregates, fine aggregates and supplementary cementitious materials were mixed for 4–5 min considering high amount of aggregates and volume of concrete. Next, water was added and again mixed for around 2–3 min until a homogenous mix was reached. The NC solution was first prepared by mixing dry NC powder with 50% of the designed water and superplasticizer in ultrasonic mixer as shown in Fig. 3 with 100% amplitude and maximum cycle for 45 min [28]. For mixes containing NC, the prepared NC solution was added in to the dry mix followed by addition of the remaining water and mixed for about 2–3 min. Slump test was performed for each mix to ensure slump values of 100–120 mm. For concrete with slump values lower than this range additional superplasticizer was added to achieve the above slump range.

Standard cylindrical specimens with diameter of 100 mm and height of 200 mm were cast for compressive strengths and durability such as sorptivity, volume of permeable voids (VPV) and rapid chloride permeability test (RCPT) based on ASTM standards. Prismatic specimens having 75 mm square cross-section and 285 mm long concrete samples with gauge studs at both ends ensuring gauge lengths of 250 mm were also cast for drying shrinkage test according to ASTM standards. All the specimens were compacted in a vibrating table with three layers for cylindrical moulds and two layers for shrinkage moulds according to the standards. All specimens were

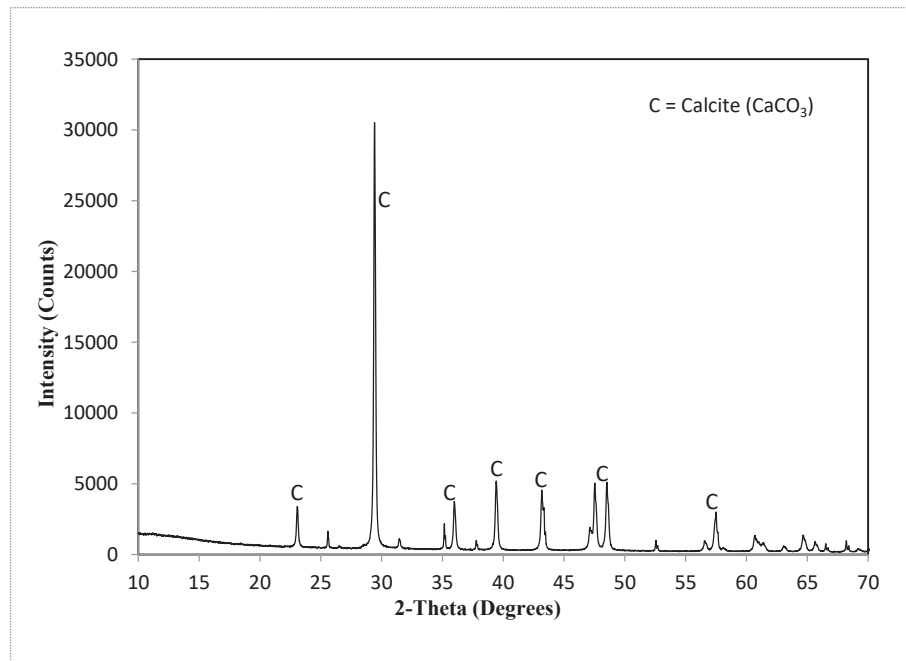


Fig. 2 – XRD analysis of nano- $\text{CaCO}_3$ .

demoulded after 24 h and the specimens were cured in lime saturated water at room temperature. For durability test such as sorptivity, VPV and RCPT, three 50 mm discs were cut from the cylindrical specimens at 28 and 90 days of concrete age and the tests were performed according to their standards. Shrinkage specimens were cured in lime saturated water in first part of curing (7 days) and then placed in a room with controlled relative humidity of 50% and at a temperature of 23 °C. The shortening readings were taken at 7, 14, 28, 35, 56, 91, 120, 150, 180, 270, 330 and 365 days of concrete age. To investigate the microstructural modifications of matrix and ITZ between aggregate and matrix of different concrete mixes due to the addition of NC, a small portion of concrete with an interfacial transition zone (ITZ) were cut from each mixes by using a diamond precision saw and dried by naturally.

#### 2.4. Testing methods

Compressive strength was measured in MATEST testing apparatus according to ASTM C873 [29] standard with a loading rate of 0.33 MPa/s until failure at 3, 7, 28, 56, 90 and 180 days of concrete age of all mixes. Diameters of the cylinders were measured and the cylinders were sulphur capped at least 4 h prior to the test. Compressive strengths were calculated as

the maximum crushing load divided by the average cross-sectional area of the specimens. For each test age, at least three specimens were tested and average value of three were reported in this study.

The rate of water absorption (sorptivity) of all concrete mixes were investigated after 28 and 90 days of water curing. At least two specimens of each concrete mix were prepared and tested according to the ASTM C1585 [30] to determine the rate of water absorption by measuring the mass of concrete specimens regularly from 1 min to 6 h and the arte of absorption ( $I$ ) was calculated by change in mass divided by cross sectional area of the specimens and the density of water.

Volume of permeable voids of 100 mm diameter and 50 mm thick specimens of all concrete mixes were measured at 28 and 90 days of concrete age according to ASTM C642 [31] standard. This test was conducted to determine the voids present in the concrete specimens and is measured by boiling the 50 mm cut concrete discs from different part of concrete cylinders at 105 °C in a water bath for at least 5 h and then weighing the samples in water. Initial weight of oven dried samples and after at least 24 h of immersion in water were measured and at least three samples were used for each concrete mixes for this test.

Table 2 – Mixing proportions of different concrete mixes ( $\text{Kg/m}^3$ ).

Mix ID	Binding Materials			nano- $\text{CaCO}_3$	Aggregates			Water
	Cement	Slag	Fly ash		Sand	20 mm	10 mm	
OPC	400	–	–	–	684	789	395	163
70BFS	120	280	–	–	684	789	395	163
69BFS.1NC	120	276	–	4	684	789	395	163
70BFS-FA	120	196	84	–	684	789	395	163
69BFS-FA.1NC	120	194	82	4	684	789	395	163





Fig. 3 – Ultra sonication of nano- $\text{CaCO}_3$ .

To determine the concrete performance against the penetration of chloride ion is known as the rapid chloride permeability test (RCPT). At least three 50 mm discs from each concrete mix after 28 and 90 days of curing period were prepared by coating them with a sealer material and then vacuum conditioning with a desiccator for at least 5 h according

to the ASTM C1202 [32] standard. Samples were then placed under water and afterwards exposed to a constant 60 voltage for 6 h on the cells in which one cell was filled with 3% NaCl solution and another cell was filled with 0.3N NaOH solution. The total charge passed through the concrete samples were collected by using a RCPT testing apparatus and average values are stated in this study.

Drying shrinkage test was performed according to ASTM C157 [33] standard. Length changes of the samples were measured at 7, 14, 28, 35, 56, 91, 120, 150, 180, 270, 330 and 365 days of concrete age in the curing room with controlled humidity and temperature. At least three samples were cast and all the specimens were measured at the same time for each concrete mix. Shrinkage strain was calculated as the difference between initial and measured length (length change) divided by the gauge length (250 mm) according to standard and average of three samples are obtained.

Microstructural investigation of high volume slag and high volume slag-fly ash blended concretes with and without NS addition was performed by using MIRA3 TESCAN SEM machine. It is a variable pressure field emission scanning electron microscope (VP-FESEM) equipped with backscattered electron (BSE) detector and energy-dispersive X-ray spectroscopy (EDS) analyser to collect SEM images along with EDS spectrum to analyse the phases. The samples were prepared by taking a small portion of dried concrete samples after 28 days of wet curing and placed them in a vacuum desiccator for minimum three days to remove all the moisture from the samples. Samples were then drenched in an epoxy resin mount, polished and then 20 mm thick carbon coat was applied to reduce the chance of getting charged during imaging and spectrum collection. The SEM and EDS were carried out at a constant accelerating voltage of 15 kV and around 15 mm of working distance by using BSE detectors for all concrete samples. SEM images and EDS spectrums were collected in and around ITZ area for each concrete mix.

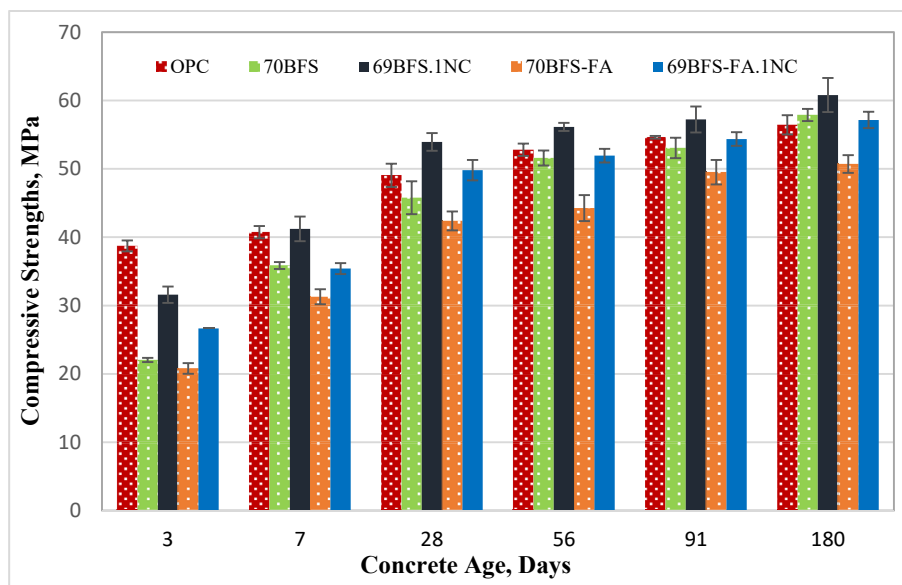


Fig. 4 – Average compressive strengths of different types concretes with and without NC at various ages of concrete.

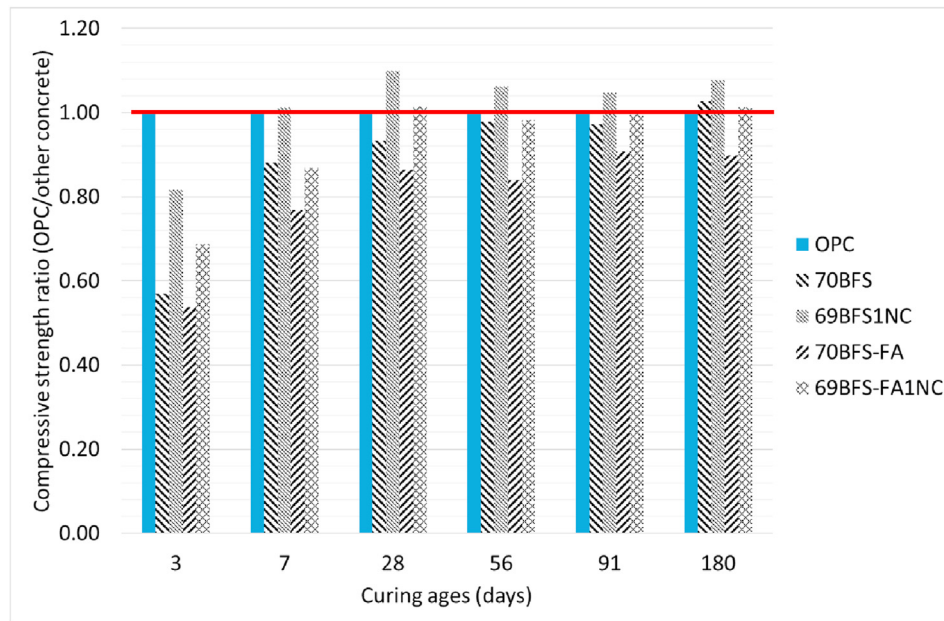


Fig. 5 – Benchmarking of compressive strength of HVS and HVS-FA concretes with control OPC concrete.

### 3. Results and discussions

#### 3.1. Compressive strengths

Average compressive strengths of control OPC concrete and concretes containing 70% BFS and combined BFS-FA blend of 70% with and without NC at the age of 3, 7, 28, 56, 90 and 180 days are shown in Fig. 4. It can be seen in the figure that the early age (3 and 7 days) compressive strength of HVS and HVS-FA concretes is very low compared to control OPC concrete and presented an increasing trend at later ages due to the slow pozzolanic reaction at early ages and then prompted at later ages of high volume BFS and FA present in those mixes which is also observed in previous studies [3,7,8,11]. It is also interesting to see in the figure that the rate of increase in compressive strength of HVS concrete containing 70% BFS is

much higher than that containing combined BFS-FA content 70%. The higher amount of CaO presents in BFS and its higher amorphous content than that of FA could be the reason for such improvement rate. It can also be seen that in high volume BFS and BFS-FA concretes the formation C–S–H is lower than that of control concrete due to lower amount of cement in formers than the latter. And due to this reason the compressive strength in those concretes at early ages i.e. 3 and 7 days is very low, but due to pozzolanic reaction additional C–S–H and C–A–H gels are formed in those concrete after 7–28 days and the rate of increase of compressive strength is faster in those concretes than that of control concrete.

It can also be noticed that the addition of 1% NC improved the early age compressive strengths significantly compared to their control concretes without NC an indication of enhanced hydration of cementitious materials facilitated by the faster

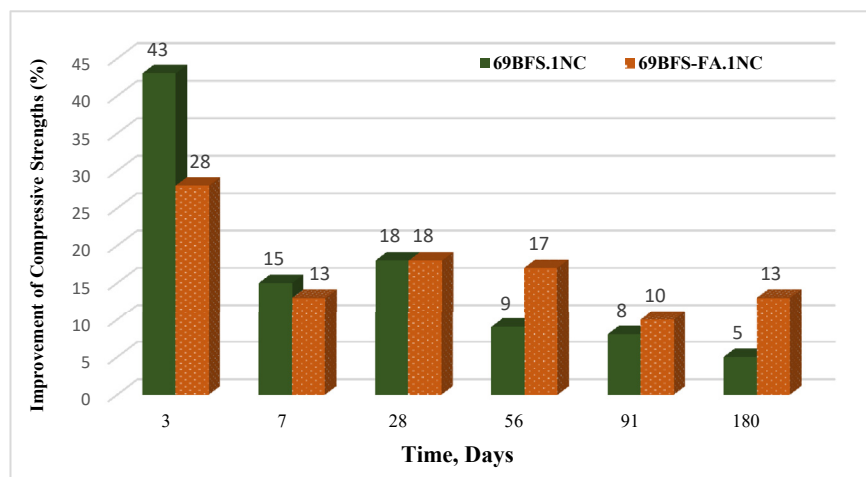


Fig. 6 – Improvement of compressive strengths of HVS and HVS-FA concretes containing 1% NC.

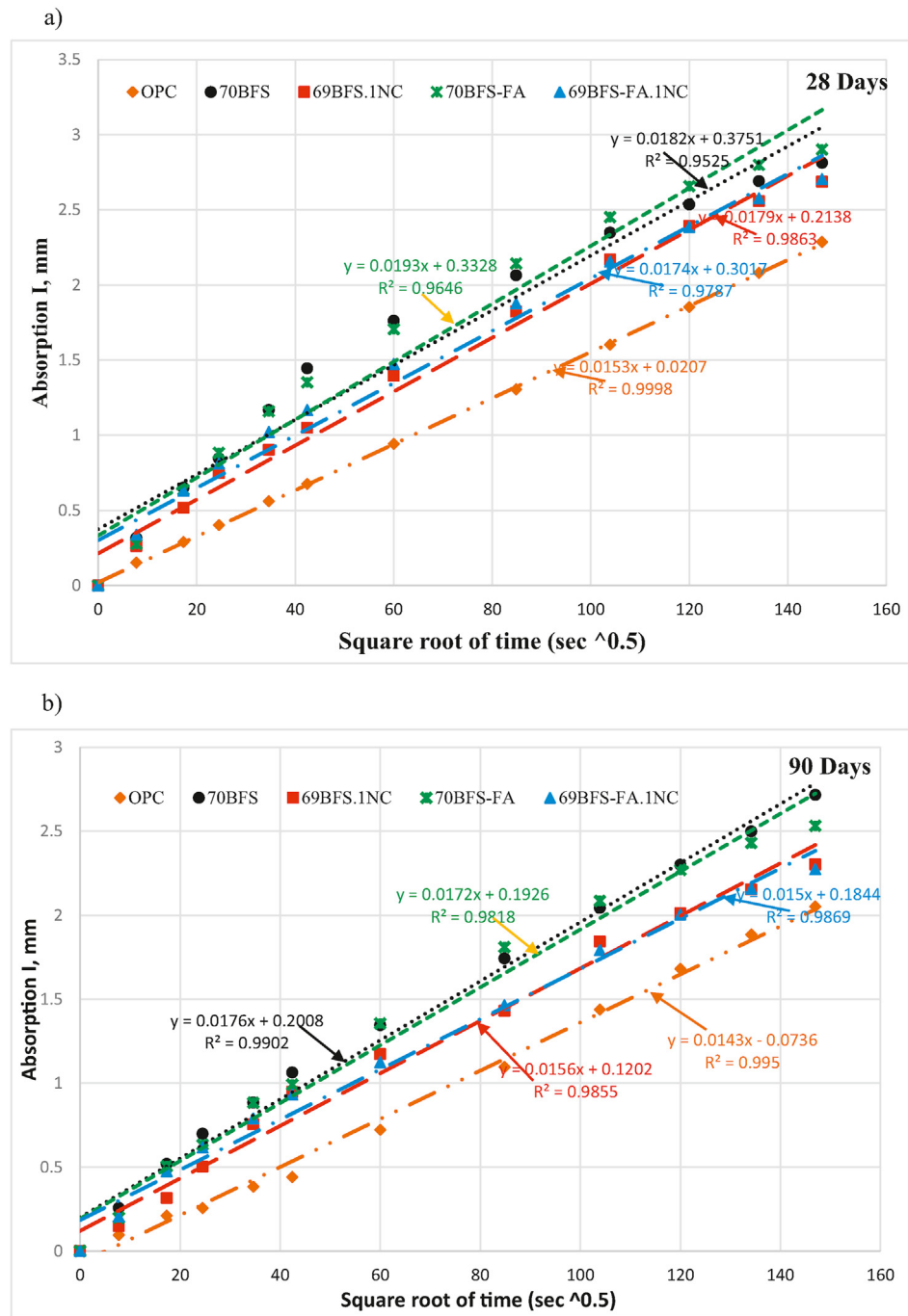


Fig. 7 – Water absorption of different type concrete with and without NC at a) 28 and b) 90 days of age.

pozzolanic reaction by NC. However, these values are still lower than the 3 days compressive strength of control OPC concrete. Interestingly, the HVS concrete containing 69% BFS and 1% NC exhibits comparable compressive strength to the OPC concrete at 7 days (see Fig. 5). This trend continues with higher compressive strength than control OPC concrete up to 6 months. It is also interesting to see that the improvement in the compressive strength of HVS-FA concrete containing 69% of BFS-FA due to addition of NC is slightly lower than the HVS concrete containing 69% BFS in early ages and exhibited higher improvement in later ages due to the presence of FA in

that mix and it reached the compressive strength of control OPC concrete at all ages. Nevertheless, both HVS and HVS-FA concretes showed higher compressive strength at later ages (28 days on wards) when benchmarked with the control OPC concrete. A very useful utilization of industrial by-products in a very high volume replacement of OPC in concrete with 54% reduced carbon footprint than the control [28].

Fig. 6 presents the percentage improvement in compressive strengths of HVS and HVS-FA concretes due to the addition of 1% NC compared to their control concretes without NC at all ages. It can be seen that the compressive strengths of

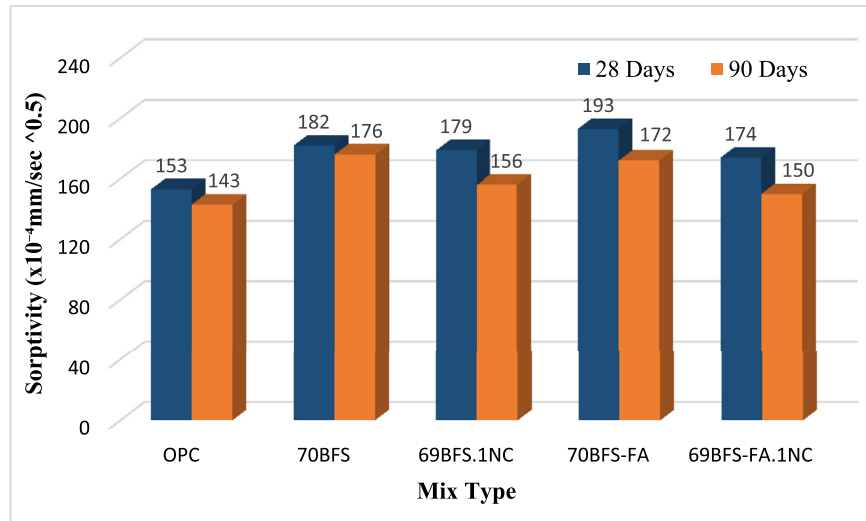


Fig. 8 – Sorptivity of different concrete mixes at 28 and 90 days.

HVS concrete containing 69% BFS is increased significantly by 43% at 3 days and 15% at 7 days due to the addition of 1% NC. However, the improvement in HVS-FA concrete containing combined BFS-FA content of 69% at early ages is not as great as HVS concrete containing 69% BFS but showed about 10–18% improvement in compressive strength from 28 days onwards. The significant increase in compressive strength of HVS and HVS-FA concretes at 3 days can be attributed to the faster pozzolanic reaction of  $\text{CaCO}_3$  nano particles with  $\text{SiO}_2$  and  $\text{Al}_2\text{O}_3$  of BFS and FA which produced additional C–S–H and C–A–H (calcium aluminate hydrate) in the matrix also showed in similar studies of high volume slag and slag-fly ash blended composites [28,35]. This has helped in reducing the porosity and densifying the matrix together with the pore filling effect of NC. The overall higher improvement in compressive strength of HVS concrete compared to HVS-FA concrete due to addition 1% NC at early ages (e.g. 3 and 7 days) can be attributed to the higher amount of CaO in BFS (about 41.2% see Table 1), which has resulted in higher amount of C–S–H in the

matrix and in the presence of  $\text{CaCO}_3$  nano particles the total ratio of Ca/Si is increased which is reflected in the EDS analysis of the matrix in the ITZ to be discussed in the microstructural analysis section. It is also interesting to see that the concrete containing same amount of combined BFS-FA showed better improvement in compressive strength development at later ages (e.g. >56 days) than that containing the same amount of BFS and equal amount of  $\text{CaCO}_3$  nano particles. This can be attributed to the slow pozzolanic reaction of FA particles than that of BFS. Slow development of compressive strength and other properties of concrete containing FA is reported by numerous researchers [8,13,14].

It can also be seen that compressive strength of 70BFS, 69BFS1NC or 69BFS-FA1NC concretes at 180 days has exceeded the compressive strength of control concrete. It can be due to the slow pozzolanic reaction of  $\text{SiO}_2$  in slag and the seeding effect of nano- $\text{CaCO}_3$ , which have contributed to the formation of additional CSH gels in those concretes at 180 days in addition to pores filling by nano- $\text{CaCO}_3$ .

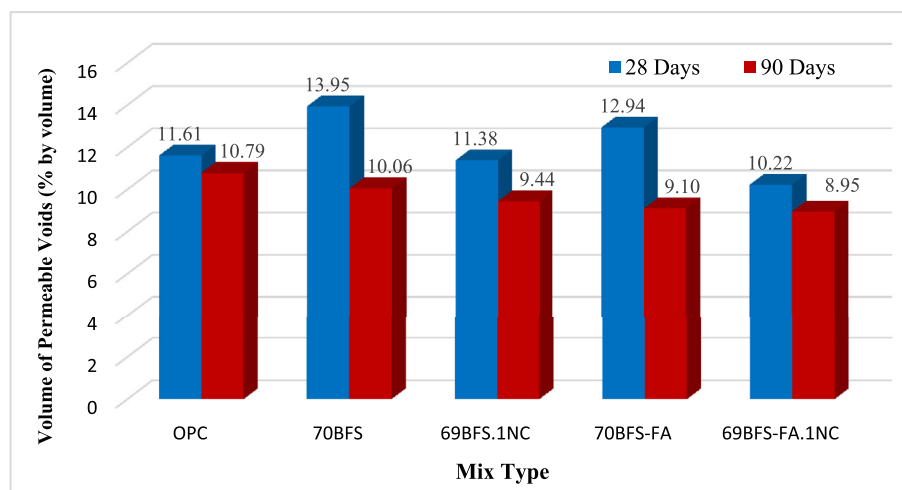


Fig. 9 – Average volume of permeable voids of concrete mixes with and without NC at 28 and 90 days.



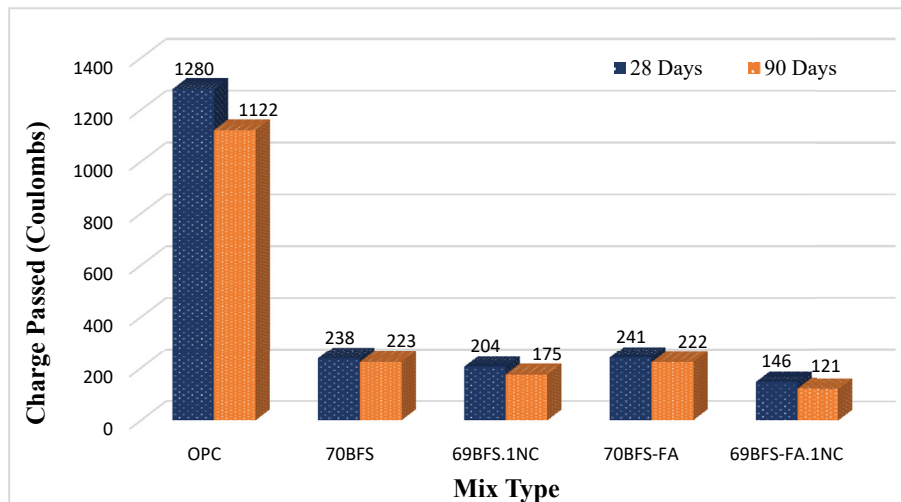


Fig. 10 – Chloride ion penetration of different concretes with and without NC at 28 and 90 days.

### 3.2. Durability properties

Fig. 7 shows the rate of water absorption of control OPC concrete, HVS and HVS-FA concretes with and without NC after 28 and 90 days of curing. The best-fit straight lines of all concrete mixes are also shown in the same figures where it can be seen that the  $R^2$  values of most of the best fit lines are greater than 0.98. The results show that the inclusion of 1% NC reduced the rate of water absorption of both HVS and HVS-FA concretes at both ages. The reduction between the HVS and HVS-FA concretes containing NC with their respective control concretes is much greater after 90 days of curing. However, the reduction is slightly higher in HVS-FA concrete than HVS concrete due to the addition of NC. The slope of the best fit lines represent the sorptivity of the concrete and is shown in Fig. 8 for all concrete mixes. It can also be seen in Fig. 7 that the sorptivity values ( $10^{-4} \text{ mm/s}^{1/2}$ ) of HVS concrete containing 1% NC are 179 at 28 days and reduced to 156 at 90 days of age which is very close to the control OPC concrete. In case of HVS-FA concrete containing 1% NC, the sorptivity values ( $10^{-4} \text{ mm/s}^{1/2}$ ) are 174 and

150 at 28 days and 90 days, respectively and also very close to the sorptivity values of control OPC concrete. It can also be seen that curing period also effected the rate of water absorption of the HVS and HVS-FA concretes containing NC than the control OPC, HVS and HVS-FA concretes without NC. The formation of additional hydration products due to pozzolanic reaction of NC, BFS and FA with cement hydration products e.g. CH and pore filling by  $\text{CaCO}_3$  nano particles might have resulted in reduced porosity of the matrix.

Volume of permeable voids of different concrete mixes with and without NC after 28 and 90 days of wet curing are shown in Fig. 9. It can be seen that the HVS and HVS-FA concretes exhibited higher volume of permeable voids than the control OPC concrete at 28 days of curing as found in other previous research studies discussed earlier. However, after 90 days of curing the permeable voids in both mixes is decreased even below the control OPC concrete and the reduction is high in HVS-FA mix. This can be attributed to the formation of more additional hydration products due to pozzolanic reaction of BFS and FA with the cement hydration products. The

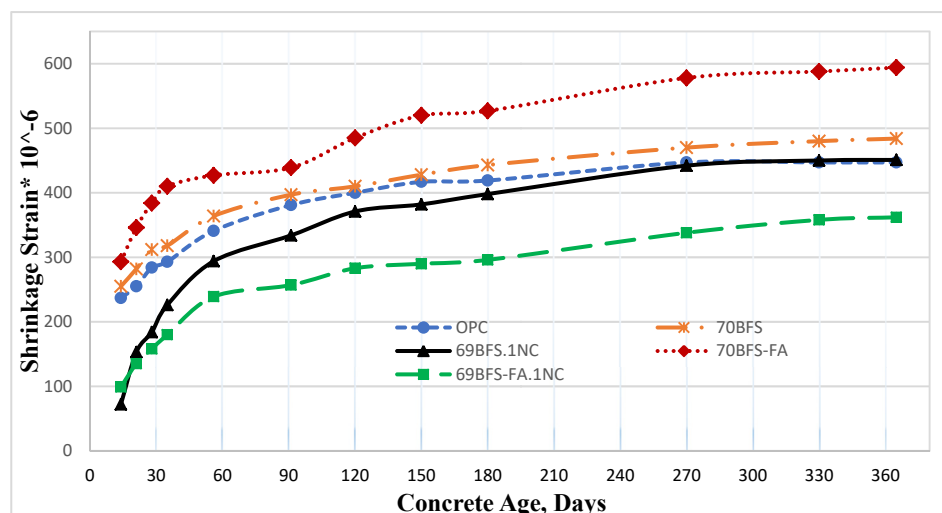


Fig. 11 – Drying shrinkage strain of control OPC, HVS and HVS-FA with and without NC at various ages of concrete mixes.

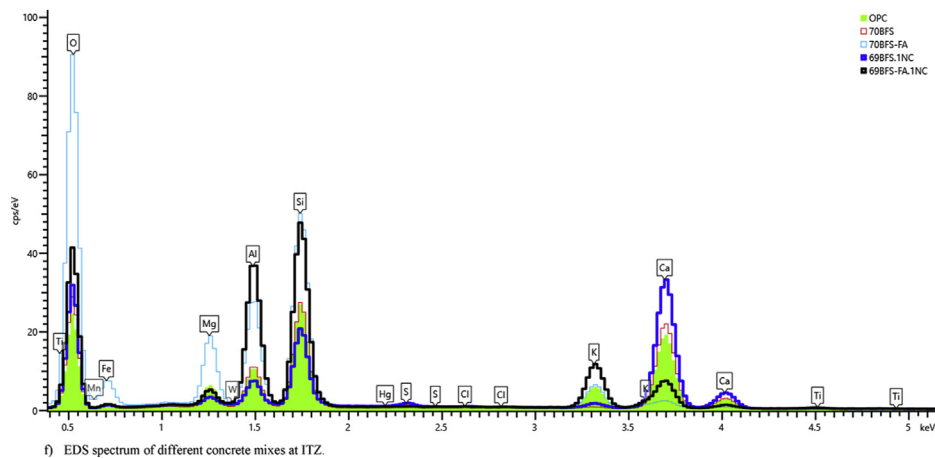
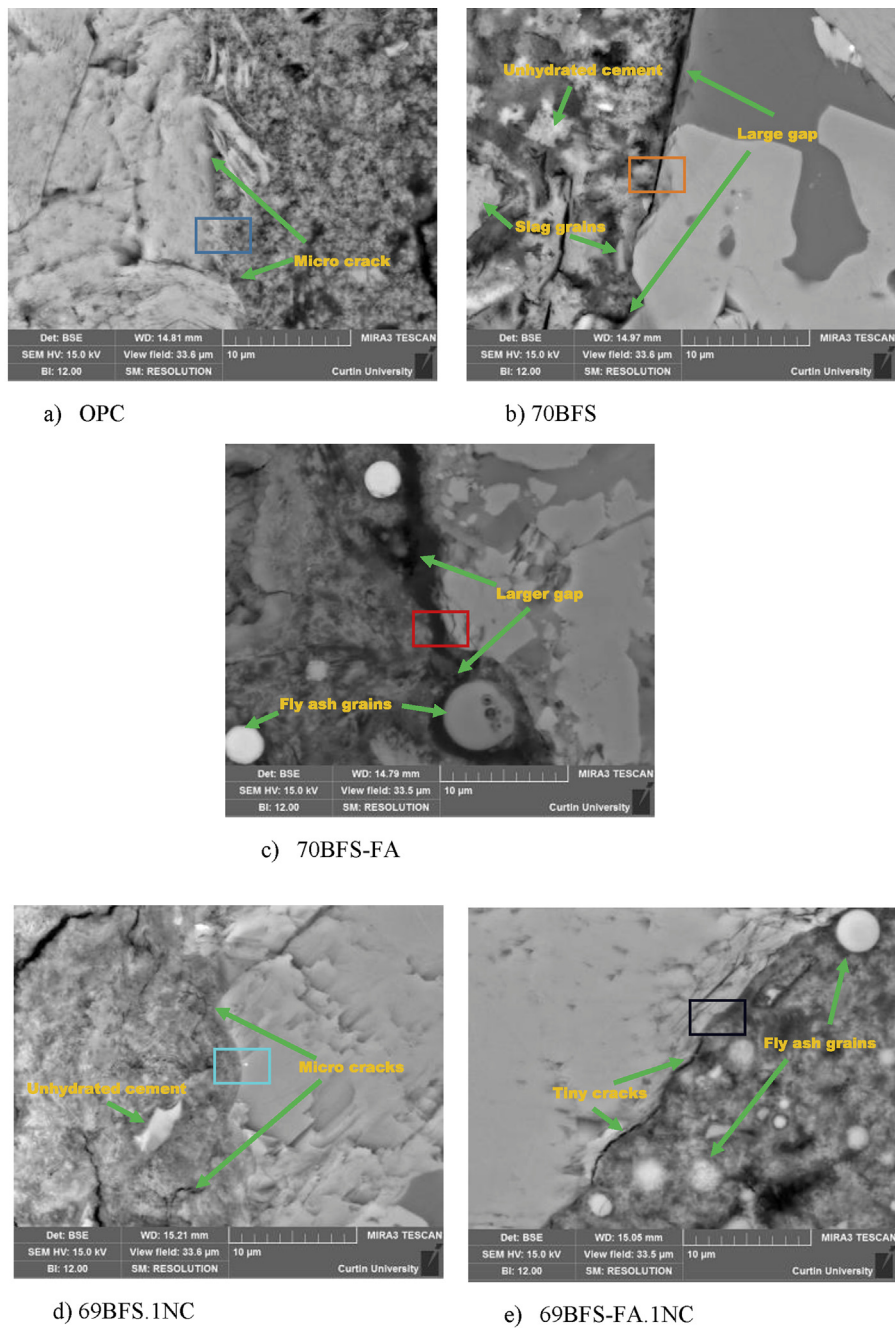


Fig. 12 – SEM images and EDS spectrum of different concrete mixes with and without nano- $\text{CaCO}_3$  addition after 28 days of curing.

beneficial effect of nano- $\text{CaCO}_3$  on the reduction of VPV of HVS and HVS-FA concretes is also evident in the same figure. It can be seen that the addition of 1% nano- $\text{CaCO}_3$  in both mixes reduced the VPV significantly by 18% and 21% than their control concretes without nano- $\text{CaCO}_3$  at 28 days of concrete age and shows slightly lower VPV than the control OPC concrete which is consistent with the strengths results of those concrete mixes. However, VPV reduction for both mixes is not great at 90 days, as just about 6% and 1% VPV is reduced at 90 days than the control HVS and HVS-FA concretes without nano- $\text{CaCO}_3$ . It can be seen that there is an inconsistency of the sorptivity and VPV values of HVS and HVS-FA concrete after 90 days curing with and without NC inclusion. It could be the reason of using two 50 mm concrete discs from the top part of the concrete cylinder for sorptivity test while four different 50 mm discs from top and bottom part of the concrete cylinder used for VPV test which resulted the average VPV values slightly lower due to the higher compactness of concrete on the bottom part of the concrete cylinders.

Fig. 10 shows the chloride ion penetration of different concrete mixes with and without nano- $\text{CaCO}_3$  at 28 days and 90 days. It can be seen that the HVS and HVS-FA concretes with or without nano- $\text{CaCO}_3$  showed outstanding resistance against penetration of chloride ion at both ages which is classified as very low level of chloride ion permeability according to ASTM C1202 standard and similar trend also found in another study [3]. It can also be seen that the addition of 1% nano- $\text{CaCO}_3$  also reduced the penetration of chloride ion and is more prominent in HVS-FA concrete in both ages, where about 39% and 45% reduction of chloride ion penetration at 28 and 90 days is observed. However, no such significant reduction observed in HVS concrete containing 70% BFS, where about 14% and 22% reduction at 28 days and 90 days, respectively is observed due to the addition of nano- $\text{CaCO}_3$ . Nevertheless, both HVS and HVS-FA concretes exhibited reduction in chloride ion penetration due to addition of 1% nano- $\text{CaCO}_3$  and exhibit very low level of chloride ion permeability. The lower charge passed through the concrete specimens is an indirect indication of denser microstructure of the matrix and the ITZ in those HVS and HVS-FA concretes.

Drying shrinkage of concrete and cement based materials is an important durability property as excessive shrinkage cause cracking of cement matrix and ITZ around aggregates. Measured shrinkage strains ( $10^{-6}$ ) of control OPC concrete, HVS and HVS-FA concrete mixes with and without nano- $\text{CaCO}_3$  addition over one year are presented in Fig. 11. It can be seen that contrary to the previous study [36] the HVS-FA concrete without nano- $\text{CaCO}_3$  exhibited higher shrinkage strain than the control OPC concrete at any age and this could be due to the presence of higher volume of slag (49% by wt.) in the mix than the volume of FA (21% by wt.) where CaO presence in the slag governed the initial hydration. However, HVS concrete containing 70% BFS showed almost similar shrinkage to the control concrete until 180 days and slightly higher shrinkage at later ages than the control OPC concrete showed consistency to the past studies [37,38] due to the higher volume of slag. The beneficial effect of nano- $\text{CaCO}_3$  inclusion in HVS and HVS-FA concretes can also be seen in the same figure. It can be seen that 1% nano- $\text{CaCO}_3$  addition reduced the early age drying shrinkage of both mixes than the control OPC

concrete as well as the HVS and HVS-FA concretes without nano- $\text{CaCO}_3$ . The most significant reduction is in HVS-FA concrete containing 69% BFS-FA and 1% nano- $\text{CaCO}_3$ . However, the reduction in drying shrinkage between the control OPC concrete and the HVS concrete containing 69% BFS and 1% nano- $\text{CaCO}_3$  decreased with the ages. The lower drying shrinkage of HVS and HVS-FA concretes containing 1% NC can be attributed to the formation of additional hydration products through pozzolanic reaction and the nano filling and seeding effect of the NC [23]. Similar reduction of drying shrinkage is also found when nano- $\text{SiO}_2$  was added with HVS and HVS-FA blended concretes [40]. The compact microstructure in those concretes containing NC yields less pores/voids and cracks and reduces the water loss through pore refining effect and hydrophilicity increasing effect [34]. The reduction of capillary pores in pastes of those HVS and HVS-FA concretes due to addition of NC observed in another study by the authors [28] is the indication of pore refinement which also helped in reducing the shrinkage of those concretes.

It can also be seen in Fig. 11 that fly ash plays different roles in high volume slag-fly ash concrete with and without nano- $\text{CaCO}_3$ . In the case without nano- $\text{CaCO}_3$ , it can be seen that the presence of fly ash in high volume slag concrete (70BFS-FA concrete) increased the drying shrinkage compared to 70BFS concrete. On the other hand, an opposite trend can be seen in the case of high volume slag and slag-fly ash concretes with nano- $\text{CaCO}_3$ . It is accepted that the pozzolanic reaction of fly ash is much slower than slag and due to this reason the microstructure of 70BFS concrete is dense than 70BFS-FA concrete. Therefore, comparatively higher porosity in 70BFS-FA concrete might have contributed higher drying shrinkage in that concrete than that of 70BFS concrete. The seeding effect of nano- $\text{CaCO}_3$  in 70BFS-FA concrete might have contributed to form higher hydration products e.g. C-S-H in this concrete than in 70BFS concrete, which eventually densified the microstructure and hence, lower drying shrinkage. Other measured durability properties and SEM images of microstructure also agree with this observation very well.

### 3.3. Microstructural modifications

The addition of 1% NC improved the compressive strength, durability properties and reduced the drying shrinkage of HVS and HVS-FA concretes. The pore filling effect of NC and formation of additional hydration products through pozzolanic reaction of NC, BFS and FA in the matrix and the densification of ITZ around the aggregates of those concretes are believed to be the reason for such improvement. Microstructure of matrix and the ITZ of all concretes in this study is studied and their SEM images and EDS spectrums are shown in Fig. 12. It can be seen in the figure that the microstructure of matrix of HVS and HVS-FA concretes (Fig. 12b-c) are relatively porous than that of concrete OPC concrete (Fig. 12a). The ITZ around the aggregate in those concretes is also porous than that of conventional OPC concrete. This can be attributed to the slow pozzolanic reaction of FA and BFS in those concretes. This observation is also consistent with the measured compressive strength, durability properties and shrinkage results. However, the

same concretes containing 1% NC show significant improvement in the microstructure of the matrix and the ITZ area as can be seen when the SEM images in Fig. 12d-e are compared with the images in Fig. 12b-c. In a recent study by the authors the improvement of modulus and hardness of matrix in the ITZ area as well as reduction of its thickness of same concretes mixes are observed using cutting age nanoindentation technique [39]. It can be seen that the microstructure of the paste matrix of concrete containing 69% BFS is significantly densified due to addition of 1% NC with very few cracks in the matrix as well as compact ITZ zone (Fig. 11d) resemble the results of similar study of HVS composites with NC [35]. Similar observation is also valid for HVS-FA concrete containing combined FA and BFS content of 69% and 1% NC. However, presence of unreacted fly ash particles can be seen in the matrix as well as few voids (Fig. 12e). Hairline cracks can also be seen in ITZ area but the ITZ zone is more compact than that observed in the HVS-FA concrete (Fig. 12c).

It can also be seen from the comparison of EDS traces taken in the ITZ of all concrete mixes that both HVS and HVS-FA concretes having higher traces of oxygen than the OPC concrete, particularly in HVS-FA concrete which is a confirmation of higher voids between the aggregates and binder paste interface of that individual concrete mix. Nevertheless, an addition of 1% nano- $\text{CaCO}_3$  in both HVS and HVS-FA mixes significantly reduces the oxygen traces and exhibited similar or even lower oxygen traces indication of higher degree of dense microstructures. Besides, an increase amount of Ca traces in those concretes is also noteworthy due to the nano- $\text{CaCO}_3$  addition in the system that point out the development of new C–S–H gel. Overall, it is clear from the microstructural investigation that the nano- $\text{CaCO}_3$  addition densified the matrix and formed a denser and compacted aggregate and binder paste interface subsequently formed a concrete with higher strengths and durability. It would be worthy to mention that EDS traces of the ITZ of selected zone (shown in Fig. 11) of different concrete mixes are compared with similar area of ITZ for all concrete mixes and compared between them to identify the differences of the spectrums found in the analysis [40].

#### 4. Conclusions

This paper presents comparable and even better compressive strength and durability properties of environmentally friendly concrete with 54% lower carbon footprint that containing 70% less OPC. Based on the results and discussions of high volume slag and high volume slag-fly ash blended concrete containing nano- $\text{CaCO}_3$ , the following conclusions can be drawn:

- ◆ The Compressive strength of high volume slag containing 69% blast furnace slag improved significantly by 43% at 3 days of concrete age due to the addition of 1% nano- $\text{CaCO}_3$  compare to their control concrete without nano- $\text{CaCO}_3$  and exceeds the compressive strengths of OPC concrete at 7 days and maintained superior strengths in the later ages.

- ◆ The addition of 1% nano- $\text{CaCO}_3$  increased the compressive strengths of high volume slag-fly ash blended concrete containing 48.5% blast furnace slag and 20.5% fly ash by 28% at 3 days of concrete age than their control concrete with no nano- $\text{CaCO}_3$  and surpasses the compressive strengths of control OPC concrete at 28 days of age and showed similar long term compressive strengths.
- ◆ Addition of 1% nano- $\text{CaCO}_3$  reduced water absorption of HVS and HVS-FA concrete by 1% and 10% respectively after 28 days of curing. However, greater reduction observed after 90 days of curing in both concretes and exhibited comparable sorptivity to control OPC concrete.
- ◆ Significant reduction of volume of permeable voids of HVS concrete containing 69% BFS and HVS-FA concrete containing 69% BFS-FA observed due to the addition of 1% nano- $\text{CaCO}_3$  by about 18% and 21% respectively than their control HVS and HVS-FA concrete after 28 days of curing and showed lower permeable voids than the OPC concrete and reduction was greater in 90 days of curing.
- ◆ Exceptional resistance against chloride ion permeability measured in HVS and HVS-FA concrete with and without nano- $\text{CaCO}_3$  addition after 28 days and 90 days of curing. Inclusion of 1% nano- $\text{CaCO}_3$  also reduced the charge passed by 14% and 22% of HVS concrete and by 39% and 45% of HVS-FA concrete than their respective control concrete after 28 and 90 days of curing respectively.
- ◆ Addition of 1% nano- $\text{CaCO}_3$  remarkably lowered the early drying shrinkage of HVS and HVS-FA concrete and maintained shrinkage strain well below in later ages of HVS-FA concrete than control OPC concrete. However, the strain reduction gap between control OPC concrete and HVS concrete containing 60% BFS and 1% nano- $\text{CaCO}_3$  was narrowing down in later ages.
- ◆ Microstructural investigation confirmed a higher degree of compacted ITZ of HVS and HVS-FA concrete due to the addition of 1% NC than the concrete without NC and possessed a similar or even better interfacial bond between aggregates and binder paste than conventional concrete.

#### Declaration of Competing Interest

The authors declare that they have no known competing financial interests or personal relationships that could have appeared to influence the work reported in this paper.

#### REFERENCES

- [1] Damtoft JS, Lukasik J, Herfort D, Sorrentino D, Gartner EM. Sustainable development and climate change initiatives. *Cement Concr Res* 2008;38(2):115–27.



- [2] Benhelal E, Zahedi G, Shamsaei E, Bahadori H. Global strategies and potentials to curb CO<sub>2</sub> emissions in cement industry. *J Clean Prod* 2013;51(Supplement C):142–61.
- [3] Elchalakani M, Aly T, Abu-Aisheh E. Sustainable concrete with high volume GGBFS to build Masdar City in the UAE. *Case Studies in Construction Materials* 2014;1:10–24.
- [4] Malhotra VM. Introduction: sustainable development and concrete technology, ACI board group on sustainable development. *ACI Concrete International* 2002;24(7):22.
- [5] Mehta PK. Reducing the environmental impact of concrete. *ACI Concrete International* 2001;23(10):61–6.
- [6] Tharakan JLP, Macdonald D, Liang X. Technological, economic and financial prospects of carbon dioxide capture in the cement industry. *Energy Pol* 2013;61:1377–87.
- [7] Duran Atiş C, Bilim C. Wet and dry cured compressive strength of concrete containing ground granulated blast-furnace slag. *Build Environ* 2007;42(8):3060–5.
- [8] Güneyisi E, Gesoğlu M. A study on durability properties of high-performance concretes incorporating high replacement levels of slag. *Mater Struct* 2008;41(3):479–93.
- [9] Oner A, Akyuz S. An experimental study on optimum usage of GGBS for the compressive strength of concrete. *Cement Concr Compos* 2007;29(6):505–14.
- [10] Wainwright PJ, Rey N. The influence of ground granulated blastfurnace slag (GGBS) additions and time delay on the bleeding of concrete. *Cement Concr Compos* 2000;22(4):253–7.
- [11] Aghaeipour A, Madhkhani M. Effect of ground granulated blast furnace slag (GGBFS) on RCCP durability. *Construct Build Mater* 2017;141:533–41.
- [12] Demirboğa R, Türkmen İ, Karakoç MB. Relationship between ultrasonic velocity and compressive strength for high-volume mineral-admixed concrete. *Cement Concr Res* 2004;34(12):2329–36.
- [13] Gesoğlu M, Özbay E. Effects of mineral admixtures on fresh and hardened properties of self-compacting concretes: binary, ternary and quaternary systems. *Mater Struct* 2007;40(9):923–37.
- [14] Kuder K, Lehman D, Berman J, Hannesson G, Shogren R. Mechanical properties of self consolidating concrete blended with high volumes of fly ash and slag. *Construct Build Mater* 2012;34:285–95.
- [15] De Weerd K, Kjellsen KO, Sellevold E, Justnes H. Synergy between fly ash and limestone powder in ternary cements. *Cement Concr Compos* 2011;41:279–91.
- [16] Sato T, Diallo F. Seeding effect of nano-CaCO<sub>3</sub> on the hydration of tricalcium silicate. *J Transportation Research Board* 2010;2141:61–7.
- [17] Pera J, Husson S, Guilhot B. Influence of finely ground limestone on cement hydration. *Cement Concr Compos* 1999;21:99–105.
- [18] Georgescu M, Saca N. Properties of blended cement with limestone filler and fly ash content. *Sci Bull* 2009;71:1454–2331.
- [19] Vishwakarma V, Sudha U, Ramachandran D, Anandkumar B, George RP, Kumari K, et al. Enhancing antimicrobial properties of fly ash mortars specimens through nanophase modification. *Mater Today: Proceedings* 2016;3(6):1389–97.
- [20] Bentz DP. Activation energies of high-volume fly ash ternary blends: hydration and setting. *Cement Concr Compos* 2014;53:214–23.
- [21] Bentz DP, Sato T, Varga ID, Weiss WJ. Fine limestone additions to regulate setting in high volume fly ash mixtures. *Cement Concr Compos* 2012;34(1):11–7.
- [22] Duran-Herrera A, De-Leon-Esquivel J, Bentz DP, Valder-Tamez P. Self-compacting concretes using fly ash and fine limestone powder: shrinkage and surface electrical resistivity of equivalent mortars. *Construct Build Mater* 2019;199:50–62.
- [23] Meng T, Yu Y, Wang Z. Effect of nano-CaCO<sub>3</sub> slurry on the mechanical properties and micro-structure of concrete with and without fly ash. *Compos B Eng* 2017;117:124–9.
- [24] Supit SWM, Shaikh FUA. Effect of nano-CaCO<sub>3</sub> on compressive strength development of high volume fly ash mortars and concretes. *J Adv Concr Technol* 2014;12(6):178.
- [25] Shaikh FUA, Supit SWM. Mechanical and durability properties of high volume fly ash (HVFA) concrete containing calcium carbonate (CaCO<sub>3</sub>) nanoparticles. *Construct Build Mater* 2014;70(Supplement C):309–21.
- [26] Shaikh FUA, Supit SWM. Chloride induced corrosion durability of high volume fly ash concretes containing nano particles. *Construct Build Mater* 2015;99:208–25.
- [27] Zhang MH, Islam J. Use of nano-silica to reduce setting time and increase early strength of concretes with high volume fly ash or slag. *Constr Build Mater* 2012;29:573–80.
- [28] Hosan A, Shaikh FUA. Influence of nano-CaCO<sub>3</sub> addition on the compressive strength and microstructure of high volume slag and high volume slag-fly ash blended pastes. *J Building Engineering* 2020;27:100929.
- [29] ASTM C873. Standard test method for compressive strength of concrete cylinders cast in place in cylindrical molds. 2015.
- [30] ASTM C1585. Standard test method for measurement of rate of absorption of water by hydraulic-cement concretes. 2013.
- [31] ASTM C642. Standard test method for density, absorption, and voids in hardened concrete. 2013.
- [32] ASTM C1202. Standard test method for electrical indication of concrete's ability to resist chloride ion penetration. 2019.
- [33] ASTM C157. Standard test method for length change of hardened hydraulic-cement mortar and concrete. 2017.
- [34] Du S, Wu J, AlShareedah O, Shi X. Nanotechnology in cement based materials: a review of durability, modeling and advanced characterization. *Nanomaterials*. 2019.
- [35] Balcikanli Bankir M, Ozturk M, Sevim UK, Depci T. Effect of n-CaCO<sub>3</sub> on fresh, hardened properties and acid resistance of granulated blast furnace slag added mortar. *J Building Engineering* 2020;29:101209.
- [36] Zhao Y, Gong J, Zhao S. Experimental study on shrinkage of HPC containing fly ash and ground granulated blast-furnace slag. *Construct Build Mater* 2017;155:145–53.
- [37] Aly T, Sanjayan JG. Mechanism of early age shrinkage of concretes. *Mater Struct* 2008;42(4):461.
- [38] Won J-P, Kim SH, Lee SJ, Choi SJ. Shrinkage and durability characteristics of eco-friendly fireproof high-strength concrete. *Construct Build Mater* 2013;40:753–62.
- [39] Hosan A, Shaikh FUA, Sarker PK, Aslani F. Nano- and micro-scale characterisation of interfacial transition zone (ITZ) of high volume slag and slag-fly ash blended concretes containing nano SiO<sub>2</sub> and nano CaCO<sub>3</sub>. *Construct Build Mater* 2020:121311.
- [40] Hosan A, Shaikh FUA. Influence of nano silica on compressive strength, durability, and microstructure of high-volume slag and high-volume slag-fly ash blended concretes. *Struct Concr* 2020:1–14. <https://doi.org/10.1002/suco.202000251>.